Ecotoxicology and Environmental Safety 162 (2018) 10–16

Contents lists available at ScienceDirect

Ecotoxicology and Environmental Safety

journal homepage: www.elsevier.com/locate/ecoenv

Novel method for *in situ* investigation into graphene quantum dots effects on the adsorption of nitrated polycyclic aromatic hydrocarbons by crop leaf surfaces

Haifeng Sun[a,b,c,*], Yanli Nan[a], Ruijie Feng[a], Ruiyao Ma[a]

[a] College of Environment and Resource, Shanxi University, Taiyuan 030006, China
[b] Department of Environmental Sciences, University of California, Riverside, CA 92521, USA
[c] Guangzhou Key Laboratory of Environmental Exposure and Health, School of Environment, Jinan University, Guangzhou 510632, China

ARTICLE INFO

Keywords:
in situ
Nitrated polycyclic aromatic hydrocarbons
Graphene quantum dots
Adsorption
Crop leaf surfaces

ABSTRACT

Nitrated polycyclic aromatic hydrocarbons (NPAHs) are PAH derivatives with more toxic effects to ecosystem, and the partitioning of NPAHs in crop system constitutes the potential exposure to human health through the dietary pathway. In the present study, a novel method for *in situ* detection of 9-nitroanthracene (9-NAnt) and 3-nitrofluoranthene (3-NFla) adsorbed onto the leaf surfaces of living soybean and maize seedlings was established based on the fiber-optic fluorimetry combined with graphene quantum dots (GQDs) as a fluorescent probe. The detection limits for the *in situ* quantification of the two adsorbed NPAHs ranged from 0.8 to 1.6 ng/spot (spot represents determination unit, 0.28 cm^2 per spot). Using the novel method, the effects of GQDs on the adsorption of individual 9-NAnt and 3-NFla by the living soybean and maize leaf surfaces were *in situ* investigated. The presence of GQDs altered the adsorption mechanism from the sole film diffusion to the combination of film diffusion and intra-particle diffusion, and shortened the time required to achieving adsorption equilibrium by 15.8–21.7%. Significant inter-species and inter-chemical variability existed in terms of the equilibrated adsorption capacity (q_e) with the sequence of soybean > maize and 3-NFla > 9-NAnt. The occurrence of GQDs enlarged the q_e values of 9-NAnt and 3-NFla by 22.8% *versus* 28.7% for soybean, and 16.2% *versus* 20.3% for maize, respectively, which was largely attributed to GQDs-induced expansion to the surface area for adsorbing NPHAs and the stronger electrostatic interaction between the -NO_2 of NPAH molecules and the functional groups (*e.g.,* -COOH, -OH) of GQDs outer surfaces. And, the varied enhancement degrees in the order of 3-NFla > 9-NAnt might be explained by the steric effects that resulted in the easier accessibility of -NO_2 of 3-NFla to the outer surface of GQDs. Summarily, the GQDs increased the retention of NPAHs on crop leaf surfaces, potentially threatening the crop security.

1. Introduction

Nitrated polycyclic aromatic hydrocarbons (NPAHs) are strong environmental mutagens and carcinogens originating from both primary emissions and secondary reactions in the atmosphere (Sun et al., 2017). Like parent PAHs (PPAHs), NPAHs are reported to be a class of semi-volatile compounds (SOCs) (Yang et al., 2017), and NPAHs have been detected in both the particulate and gaseous phases of combustion emissions and the ambient atmosphere. More remarkably, studies have shown that the occurrence of NPAHs in ambient air is 10–100 times lower than those of their PPAHs, but their toxicity is 10–100,000 times higher than that of PPAHs (Fujii et al., 2017; Gao et al., 2018). Living plant cuticles can enrich hydrophobic SOCs mainly from the atmosphere due to the presence of hydrophobic wax layer, which strongly affect the fates of SOCs (Barber et al., 2002; Su and Wania, 2005; Li et al., 2009). Meanwhile, the SOCs adsorption by crop or vegetation leaf cuticles also constitutes a direct exposure pathway to human health (Desalme et al., 2013). Recently, we *in situ* investigated the uptake of parent and alkylated PAHs by crop leaf surfaces, as well as the effects of surfactants (Sun et al., 2018a). NPAHs have been detected in plant materials, such as tree barks, tea leaves, fresh parsley, *etc.* However, few studies have delved into the adsorption of gaseous NPAHs by living crop leaf surfaces.

As a matter of zero-dimensional luminescent carbon-based nanomaterials, graphene quantum dots (GQDs) can be viewed as a scaled down version of graphene oxide (GO), and also as an enlargement of

* Corresponding author at: College of Environment and Resource, Shanxi University, Taiyuan 030006, China.
E-mail address: hfsun86@sxu.edu.cn (H. Sun).

https://doi.org/10.1016/j.ecoenv.2018.06.059
Received 28 March 2018; Received in revised form 19 June 2018; Accepted 20 June 2018
Available online 26 June 2018
0147-6513/ © 2018 Elsevier Inc. All rights reserved.

benzene-based molecules, *i.e.,* PAHs (Li et al., 2013, 2017). Emerging as superior functional materials, GQDs have received extensive attention in various studying areas, including biological, environmental and energy-related applications (Zhang et al., 2012; Sun et al., 2014; Sahub et al., 2018). With such promising potential for considerable applications, GQDs would be released into the environment and transported between environmental media inevitably, which may trigger uncertain ecological effects (Lin et al., 2014). Recently, we observed that the presence of graphene (GNS) and GO nanosheets inhibited the total depuration of PPAHs from the living spinach leaf surfaces (Sun et al., 2018b). However, the effects of GQDs on the adsorption of gaseous NPAHs by living crop leaf surfaces are poorly understood.

A variety of analytical methods have been established for the measurement of NPAHs levels in environmental samples, such as GC/MS, LC/ECD, GC/TOFMS, *etc.* (Domeño et al., 2012; Fujii et al., 2017; Li et al., 2016). As is well known, these methods are accompanied with destructive pretreatments (extraction and separation), which might destroy the original forms and eliminate the spatial distributions of NPAHs in/on plant tissues in unknown ways. Therefore, the development of *in situ* method for direct determination of NPAHs on crop leaf surfaces is of great necessarily. By far, some *in situ* approach have been established to determine the PPAHs levels adsorbed on the plant leaf surfaces, such as solid surface fluorescence, laser-induced nanosecond time-resolved fluorescence, and fiber-optic fluorimetry (FOF) (Wang et al., 2008; Sun et al., 2016), *etc.* Although fluorescent response of NPAHs is relatively lower than that of PPAHs due to the high electron-withdrawing nitro-group, Guiñez et al. (2017) established a novel method for the quantification of 9-nitroanthracene (9-NAnt), and 3-nitrofluoranthene (3-NFla) in water samples based on molecular fluorescence detection. Therefore, the suitability of existing methods for the *in situ* determination of NPAHs on crop leaf surfaces is worthy of attention. Additionally, due to the high fluorescence yield, GQDs have attracted considerable attention in the determination of biological and chemical substances (Liu et al., 2017; Achadu and Nyokong, 2017; Luo et al., 2018). Recently, a novel fluorescence quenching method for *in vivo* quantification of N/O/S-containing PAHs (dibenzothiophene, carbazole and dibenzofuran) retained on the mangrove root epidermis using GQDs as a fluorescent probe (Li et al., 2018). However, the question of whether it could realize the *in situ* quantification of NPAHs adsorbed onto the living crop leaf surfaces using GQDs as a fluorescent probe remain unclear.

In this work, 9-NAnt and 3-NFla were selected as the model components of NPAHs owing to their relative prevalence in gas phase. Soybean and maize were chosen as the studying focuses due to the most commonly consumed crops around the world. The overall objectives of the present study were to develop a novel method for *in situ* determination of NPAHs adsorbed onto the living soybean and maize leaf surfaces based on GQDs as a fluorescent probe, and to *in situ* determine the effects of GQDs on the adsorption kinetics of gaseous NPAHs by the two crop leaf surfaces.

2. Materials and methods

2.1. Apparatus and reagents

A standard sample of 9-NAnt (purity > 95%) was supplied from Sigma-Aldrich Co. Ltd. (UK) and 3-NFla (purity > 95%) from AccuStandard Inc. (USA). In this study, The GQDs with the diameter ~3 nm were purchased from J&K Scientific Co. Ltd. (USA). All of the other chemicals (A.R.) were obtained from Shanghai Trustin Chemical Co., Ltd (China). Stock solutions of NPAHs at 500 μg/L were prepared in methanol and stored at − 20 °C before use. GQDs solutions dispersed in methanol were prepared and then sonicated for 10 min, followed by incubation on the bench overnight. The dispersions of GQDs in methanol were monitored using the zeta potential, and the value was smaller than − 45 mV, indicating that GQDs colloidal particles had good stability and carried negative charge.

Fluorescence spectra of NPAHs and GQDs were all *in situ* recorded on a Cary Eclipse fluorescence spectrophotometer equipped with fiber-optic accessories of 2-m length and 150-W Xenon lamp (Agilent, USA) (Fig. S1). During the measurement, the excitation and emission slits were fixed at 10 nm and 5 nm, respectively; PMT voltage was 600 V and the scan rate was set as 12,000 nm/min; an angle between the fiber-optic probe and the tested crop leaves was kept at 45° to avoid the interference from the scattered light (Fig. S1). 10-μL flat head micro-injections (Shanghai Medical Laser Instrument Plant, China) that used for introducing NPAHs and GQDs solution onto the soybean and maize leaf surfaces. The stomatal conductance of two crop leaves with and without GQDs pressure was measured using a Delta-T AP4 leaf porometer (Barber et al., 2002).

2.2. Preparation and pretreatment of living crop seedlings

The plants were cultured for 21 days in a controlled climate chamber (MGC-450HP, Shanghai Yiheng Science Instruments Co. Ltd., China): light irradiation was set for 12 h light (18,000 lx) and 12 h dark, and temperatures were set at 24 °C during light period and 22 °C during dark regime, with relative humidity of 55%. Then, the seedlings with similar growing stage (5–6 leaves) and biomass were obtained from the cultured plants for the following adsorption experiments. Next, the silts adhered onto the leaf surfaces were washed off successively with tap water and Milli-Q water three times. Finally, the determination areas evenly distributed on the front, middle and nether of leaf surfaces were produced using a large circle end of 5-mL pipette based on the method as recorded by Sun et al. (2016). The area of the circle (0.28 cm^2, r ≈ 0.30 cm) was marked as a unit of 'spot', basically having the same area as the fiber-optic probe, which has been displayed visually in Fig. S1.

2.3. Quantification of NPAHs adsorbed onto the crop leaf surfaces

For the seedlings without GQDs treatment, the fluorescence spectra of 9-NAnt and 3-NFla with five concentration gradients ranging from 0 to 400 ng/spot and 0–500 ng/spot, respectively, were directly obtained using the FOF method, and the operations were consistent with what were recorded in our previous studies (Sun et al., 2016, 2018a). For the GQDs-treated seedlings, the GQDs solutions were introduced onto the 'spots' to produce the dosages of 100 ng/spot. Two hours later, respective 9-NAnt and 3-NFla solutions with five concentration gradients ranging from 0 to 400 ng/spot and 0–300 ng/spot were introduced onto these 'spots' interacted with GQDs. After the complete evaporation of methanol, the fluorescence spectra of GQDs were acquired between 380 and 550 nm wavelength range at the excitation wavelength (λ_{ex}) of 325 nm using the FOF method.

2.4. Adsorption experiment

In the present study, 'seedlings without GQDs treatment' and 'seedlings treated with GQDs' referred to the control and experimental group, respectively. For each item, three replicate seedlings and three replicate leaves (one per seedling) were selected for the adsorption experiment. Firstly, 100 ng/spot dosages of GQDs were introduced onto the 'spots' on the leaf surfaces of living soybean and maize seedlings. Two hours later, the seedlings treated with/without GQDs were all transferred into a 125-L exposure chamber to perform adsorption experiment. The controlled exposure chamber was basically the same as that used in our previous study (Sun et al., 2018a) with minor modifications. Briefly, the key parameters were set as follows: light/dark regime, 16/8 h; temperature: (23 ± 2) °C; relative humidity: (40 ± 3)%; illumination intensity: 18000 lx. The contaminated air was produced based on the method reported by Sun et al. (2016): approximately 10 mg of individual 9-NAnt and 3-NFla were dissolved in

10 mL methanol in a 50-mL brown bottle with an inlet and an outlet. According to the method reported by Sun et al. (2018a), a stable and elevated concentration (147 ± 12 ng/m^3) of gaseous NPAHs was produced in the chamber. Finally, fluorescence intensity of NPAHs adsorbed by the leaf surfaces of living soybean and maize seedlings was *in situ* obtained at the setting time points.

2.5. Statistical analysis

For each item, the mean values of nine measurements was presented as the final results, and a non-parametric Kruskal-Wallis test was applied for comparison of the experimental results. The significance for all tests is evaluated at the 95% confidence level ($P < 0.05$).

3. Results and discussion

3.1. Analytical merits of NPAHs determination without GQDs

Firstly, the fluorescence spectra for the *in situ* detection of the two adsorbed NPAHs without GQDs were optimized using the FOF method. In the absence of the GQDs, the optimal λ_{ex} and emission wavelengths (λ_{em}) of 9-NAnt and 3-NFla were 257/405 nm and 280/462 nm for soybean; 258/407 nm and 282/461 nm for maize, respectively. Notably, the fluorescence intensity (I) escalated with the concentration of NPAHs (C_{NPAHs}) adsorbed onto the two crop leaf surfaces, and a strong positive correlation were observed between I values and C_{NPAHs} with good correlation coefficients > 0.99 (Fig. S2). Table S1 displays the analytical merits for the *in situ* determination of 9-NAnt and 3-NFla adsorbed onto the leaf surfaces of two crop seedlings. It can be seen that the detection limits for the *in situ* quantification of adsorbed 9-NAnt and 3-NFla varied in the range of 7.8–11.9 ng/spot, respectively. Consequently, within a certain range, the FOF method was capable of *in situ* quantifying the amount of NPAHs adsorbed onto the two crop leaf surfaces. In our previous study, a FOF method was established for the *in situ* determination of Fla adsorbed onto the mangrove leaf surfaces, with the detection limits as low as 0.9 ng/spot (Sun et al., 2016). Obviously, the sensitivity of the FOF method for the *in situ* detection of NPAHs was much lower than that of corresponding PPAHs. The observation could be explained by the fact that the high electron-withdrawing effects of nitro-group weakened the fluorescent response of NPAHs compared to corresponding PPAHs (Chen et al., 2015; Li et al., 2018). However, the amount of NPAHs accumulated on/in the plant leaves is much lower than that of PPAHs in a real environment (Musa Bandowe and Meusel, 2017). Therefore, the development of a novel *in situ* method with high sensitivity and accuracy is urgent.

3.2. In situ measurement of NPAHs with GQDs

3.2.1. Characterization of GQDs

Fig. S3 displays the transmission electron microscopy (TEM) image of GQDs. It could be seen that GQDs was basically spherical in shape with a diameter of approximately 3 nm and mostly uniform in size. From Fig. 1a, the FTIR spectra of GQDs show a broad adsorption band at ~3214 cm^{-1}, corresponding to the stretching vibration of O-H functional groups at the edges. The sharp peaks at 1716 cm^{-1} and 1642 cm^{-1} were attributed to the stretching mode of C=O and C=C bonds, respectively. In addition, the peaks at 1385 cm^{-1} and 1071 cm^{-1} were assigned to the stretching vibration of carboxyl O=C–O and alkoxy C–O bonds, respectively (Shehab et al., 2017). Raman spectroscopy (Fig. 1b) describes the quality of the GQDs used in the present study. The major Raman features refers to the D band and G band at around 1350 cm^{-1} and 1584 cm^{-1}, respectively. The relative intensity of the 'disorder' D-band to the crystalline G- band (I_D/I_G) for the used GQDs is approximately 0.65, indicating the high quality of GQDs with few layer graphene nanoribbons (Li et al., 2011). According to Brunauer-Emmett-Teller (BET) method (Doroodmand and Deylaminezhad, 2015), the specific surface area of GQDs was determined with the average value of 24.8 m^2/g.

3.2.2. Analytical merits of the proposed method

The fluorescence spectrum of GQDs on the soybean leaf surfaces recorded at a λ_{ex} of 325 nm is shown in Fig. 2a, and the spectra of GQDs show an emission peak in the visible spectrum at 461 nm. Typically, the luminescence mechanism of GQDs relies on intrinsic state emission and defect state emission (Zhu et al., 2012). Additionally, the relative fluorescence intensity of GQDs decreased gradually with the increasing concentration of 9-NAnt on the soybean leaf surfaces. Specifically, the measurement of the fluorescence lifetime of GQDs with and without quencher molecules is one of the most useful way to distinguish static quenching from dynamic quenching. Under the optimal experimental conditions, the fluorescence lifetime of GQDs was calculated to be 3.76 ns without NPAHs, and the values were 3.74 ns and 3.72 ns in the presence of 9-NAnt and 3-NFla, respectively (Fig. S4). There was no significant difference between the two groups of values ($P > 0.05$), indicating that the fluorescence quenching of GQDs induced by NPAHs is a static quenching process, rather than dynamic quenching. In brief, given the presence of conjugated system, the static quenching effects were mainly due to both the π-π stacking interactions and the hydrophobic interactions between GQDs and NPAHs (Wang et al., 2017).

To better display the fluorescence quenching effects and further develop the *in situ* method, the Stern-Volmer equation was used as follows:

$$I_0/I = 1 + K_{SV}{}^{*}C_{NPAHs} \quad (1)$$

I_0 and I represent the fluorescence intensity of GQDs on the soybean leaf surfaces in the absence and presence of NPAHs, respectively; K_{SV} refers to the Stern-Volmer quenching constant, and C_{NPAHs} is the concentration of NPAHs adsorbed onto the leaf surfaces of living soybean and maize seedlings. From Fig. 2b, the quenching degree (I_0/I) at the optimal wavelength escalated with the increasing content of 9-NAnt

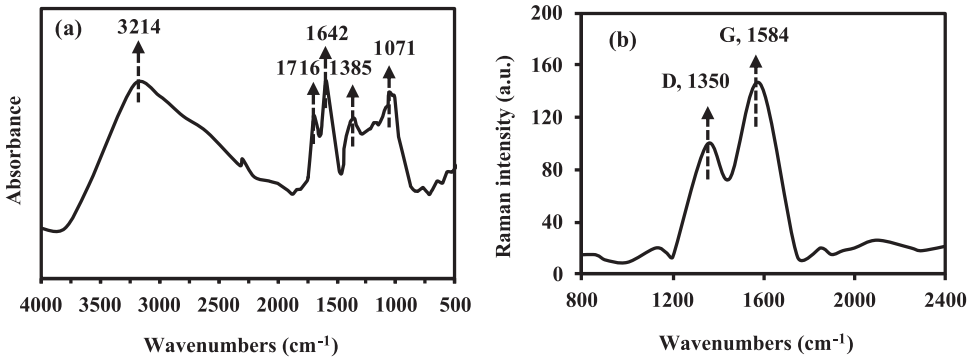

Fig. 1. Characterization of GQDs: (a) FTIR spectra; (b) Raman spectra.

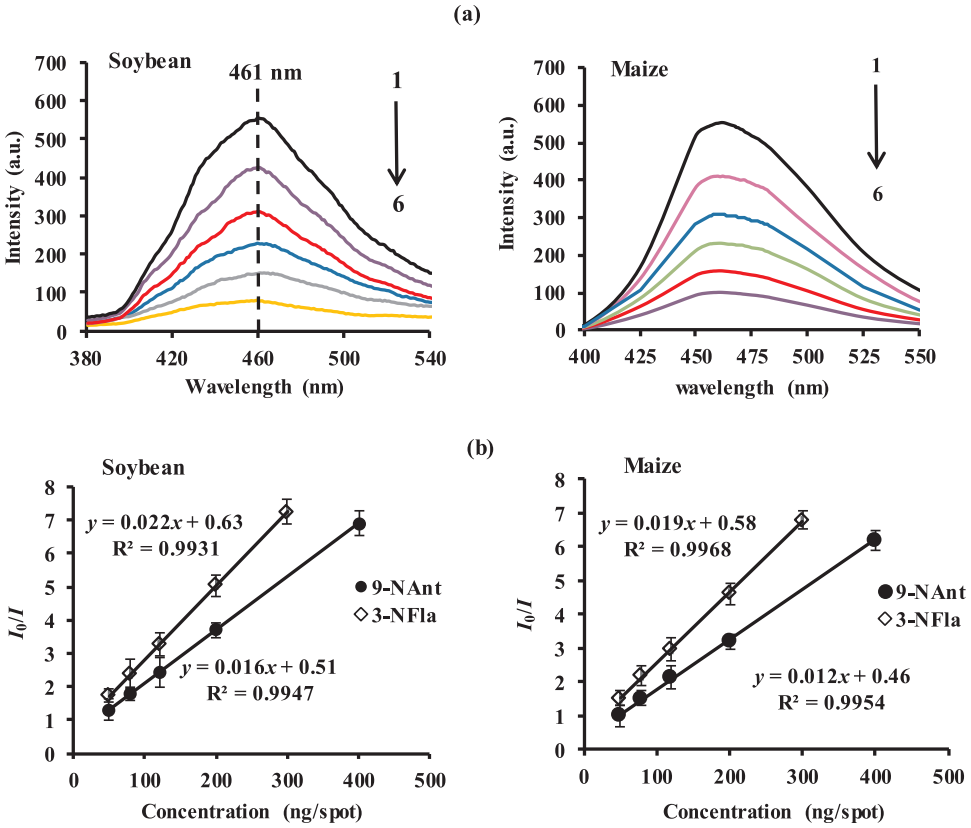

Fig. 2. (a) The variation in the fluorescence spectra of the GQDs (100 ng/spot) with the increasing concentrations of 9-NAnt (1–6: 0, 50, 80, 120, 200, 400 ng/spot) on the soybean and maize leaf surfaces, respectively. (b) The linear relationship between I_0/I and the concentration of NPAHs. Each emission spectrum is the mean of nine replicates.

Table 1
Analytical merits of the novel method based on GQDs (100 ng/spot) as fluorescent probe (n = 9).

Crop	NPAHs	Linear regression equations	Linear ranges (ng/spot)	Correlation coefficients	Detection limits[c] (ng/spot)
Soybean	9-NAnt	y[b] = 0.016x[a] + 0.51	2.9–410	0.9947	1.4
	3-NFla	y = 0.022× + 0.63	1.7–370	0.9931	0.8
Maize	9-NAnt	y = 0.012× + 0.46	3.4–435	0.9954	1.6
	3-NFla	y = 0.019× + 0.58	2.1–390	0.9968	1.2

[a] x is the concentration of NPAHs adsorbed onto the crop leaf surfaces.
[b] y represents the I_0/I values of GQDs on the leaf surfaces.
[c] detection limits that are calculated by $3S_B/k$, where 'S_B' is the standard deviation of the blank (n = 9), and 'k' is the slope of the calibration curve.

and 3-NFla adsorbed on the soybean and maize leaf surfaces, respectively. Obviously, a strong positive correlation was observed between the I_0/I values and C_{NPAHs} within certain concentration ranges. Using the novel method, the analytical merits for the *in situ* quantification of NPAHs adsorbed onto the living soybean and maize leaf surfaces were determined and the experimental results are present in Table 1. The linear ranges of 9-NAnt and 3-NFla were 2.9–410 ng/spot and 1.7–370 ng/spot for soybean, 3.4–435 ng/spot and 2.1–390 ng/spot for maize, respectively. More importantly, the detection limits can reach as low as 1.4 ng/spot and 0.8 ng/spot for 9-NAnt and 3-NFla, respectively. Obviously, the sensitivity of the novel method was approximately 8–10 times higher than that of the FOF method, which opens a more promising analytical platform for the *in situ* determining the occurrence of NPAHs in crop system. For further verifying the feasibility and accuracy of the newly method, the recovery experiment was performed and the recoveries ranged from 84.1% to 113.9% (Table S2). Meanwhile, the relative standard deviations (%RSD) were less than 7.3%. All the observations clearly confirmed the feasibility of the developed method for the *in situ* measurement of adsorbed NPAHs on the crop leaf surfaces.

3.3. Adsorption of NPAHs by the crop leaf surfaces

3.3.1. Adsorption kinetics

The mechanism controlling the adsorption of gaseous NPAHs by the leaf surfaces of two living crop seedlings was further determined by modeling the adsorption kinetics of the processes. The data shown in Fig. 3 was analyzed using two classic kinetic models shown as follows (Konggidinata et al., 2017):

The pseudo-first-order equation:

$$\ln (q_e - q_t) = \ln q_e - k_1 t \quad (2)$$

The pseudo-second-order equation:

$$t/q_t = 1/k_2 q_e^2 + t/q_e \quad (3)$$

In the equations, q_e and q_t (ng/spot) represent the amounts of adsorbed NPAHs at equilibrium and at any time t (h), respectively; k_1 and k_2 are the rate constants of the pseudo-first-order and pseudo-second-order equations, respectively.

Clearly, for the seedlings without and with GQDs treatment, the experimental data exhibited poor correlation to the pseudo-first-order model, with fitting coefficients (R^2) < 0.63 (Table 2). Moreover, the calculated q_e values from the equation for 9-NAnt and 3-NFla did not match the experimental data (P < 0.05). Consequently, pseudo-first-order model failed to describe the adsorption processes of the two NPAHs by the two crop leaf surfaces. In contrast, the pseudo-second-order equation offered excellent agreement with the experimental values for two selected NPAHs, as evidenced by the good R^2 (> 0.91) of determination for the linear regression (Table 2). The good fitting of the experimental data to the model might describe the chemisorption

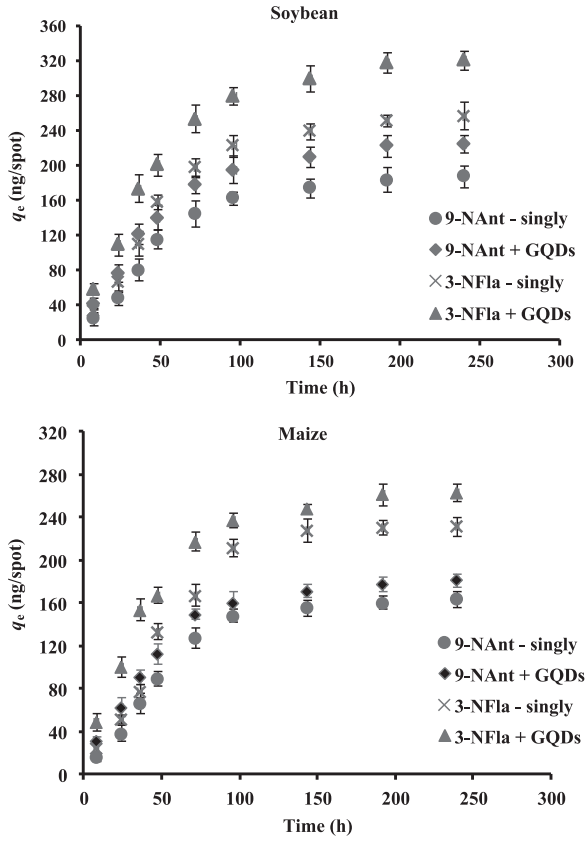

Fig. 3. The adsorption kinetics of NPAHs on the leaf surfaces of living crop seedlings, and the concentration of GQDs was 100 ng/spot. Results are shown as means ± SD (n = 9).

nature of the two NPAHs by crop leaf surfaces to some extent (Sham and Notley, 2018). The pseudo-second-order model also predicted the equilibrated adsorption capacity (q_e) of 9-NAnt and 3-NFla accurately, with < 8.9% difference between the experimental and calculated q_e values.

In case of GQDs-treated seedlings, there also existing some dissimilarity from the ones without GQDs treatment. Summarily, one of the noticeable effects induced by GQDs on the adsorption kinetics of NPAHs is the variations in the R^2 values. It is noted that, for pseudo-second-order equation, the R^2 values of the NPAHs coexisted with GQDs (> 0.95) became greater than that without GQDs. As reported, the pseudo-second-order model is based on the assumption that the rate-limiting step may be chemical interaction during the sorption process (Su et al., 2011; Chen et al., 2014), thus the results indicated that the presence of GQDs enhanced the nature of chemisorption. The other GQDs-induced effect on adsorption processes is the significant variation of the k_2 values corresponding to pseudo-second-order equation (Table 2) ($P < 0.05$). The k_2 values of 9-NAnt and 3-NFla increased by 22.9% and 16.7% for soybean, 20.5% and 13.1% for maize, respectively, with the addition of GQDs, suggesting that the presence of GQDs accelerated the adsorption of NPAHs by the living soybean and maize leaf surfaces. Ying et al. (2016) reported the adsorption

capacity of GNS modified by GQDs for toxic organic contaminants. A record-breaking adsorption rate was demonstrated and the enhancement in performance by nearly a factor of three compared to that of GNS was attributed to the greatly increased accessible surface area of GNS. Consequently, it was assumed that the addition of GQDs would expand the surface area of soybean and maize leaf surfaces for adsorbing gaseous NPAHs, thereafter enlarging the k_2 values to some extent. The assumption could be further verified by the variation of stomatal conductance caused by the presence of GQDs. Specifically, the

Table 2
Effects of GQDs on kinetic parameters for adsorption of NPAHs on the living crop leaf surfaces.

Models	Parameters	Soybean				Maize			
		9-NAnt		3-NFla		9-NAnt		3-NFla	
		single	GQDs	single	GQDs	single	GQDs	single	GQDs
Pseudo-first- order	$q_{e,\ calc}$ (ng/spot)	351.8 ± 17.6^a	529.4 ± 31.8^b	432.5 ± 21.7^a	604.7 ± 51.4^a	318.4 ± 19.1^a	433.9 ± 52.1^c	394.2 ± 26.8^a	465.0 ± 33.6^b
	$q_{e,\ exp}$ (ng/spot)	199.7 ± 12.0^a	245.2 ± 15.9^b	273.4 ± 17.2^a	351.9 ± 17.6^a	155.3 ± 18.4^b	180.5 ± 9.6^a	217.6 ± 23.9^b	261.8 ± 15.7^a
	k_1	− 0.35 ± 0.017^a	− 0.72 ± 0.043^b	− 0.21 ± 0.012^b	− 0.58 ± 0.039^c	− 0.27 ± 0.017^a	− 0.65 ± 0.033^b	− 0.18 ± 0.010^a	− 0.49 ± 0.028^a
	R^2	0.5159	0.4627	0.4903	0.5681	0.6276	0.5795	0.6084	0.5392
Pseudo-second-order	$q_{e,\ calc}$ (ng/spot)	187.5 ± 10.6^a	225.9 ± 13.4^a	256.4 ± 17.2^a	320.6 ± 24.8^b	162.7 ± 9.6^a	179.3 ± 10.7^b	230.8 ± 14.5^a	265.1 ± 19.3^a
	$q_{e,\ exp}$ (ng/spot)	199.7 ± 11.5^a	245.2 ± 14.9^a	273.4 ± 15.4^a	351.9 ± 21.6^c	155.3 ± 12.1^a	180.5 ± 12.2^a	217.6 ± 11.7^b	261.8 ± 17.8^a
	k_2	0.0048 ± 0.0002^a	0.0059 ± 0.0003^a	0.0042 ± 0.0002^b	0.0049 ± 0.0002^a	0.0035 ± 0.0001^a	0.0042 ± 0.0002^a	0.0031 ± 0.0002^a	0.0035 ± 0.0002^a
	R^2	0.9275	0.9563	0.9190	0.9685	0.9113	0.9644	0.9175	0.9524
Film diffusion	B	− 0.019 ± 0.001^b	− 0.016 ± 0.001^a	− 0.017 ± 0.002^a	− 0.014 ± 0.001^b	− 0.015 ± 0.0009^a	− 0.011 ± 0.001^b	− 0.012 ± 0.0008^a	− 0.009 ± 0.0009^a
	R^2	0.9653	0.8279	0.9598	0.7941	0.9475	0.8523	0.9446	0.8194
Intra-particle Diffusion	k_p	5.37 ± 0.2^a	8.92 ± 0.5^a	3.64 ± 0.3^a	7.15 ± 0.4^a	4.26 ± 0.2^a	7.68 ± 0.5^a	3.93 ± 0.1^a	6.84 ± 0.4^a
	C	104.6 ± 3.6^a	151.7 ± 2.8^a	126.3 ± 2.1^a	179.6 ± 3.1^a	61.5 ± 1.8^a	90.8 ± 2.3^a	99.2 ± 2.1^a	132.7 ± 3.4^a
	R^2	0.2726	0.7991	0.2458	0.7517	0.1982	0.8035	0.2684	0.7846

The results are shown as the means ± SD of nine replicates for each treatment. For each item, means superscripted by the different lower-case letters in a column indicate significant differences ($P < 0.05$) between the treatments based on the determination by Kruskal-Wallis test.

average stomatal conductance under the pressure of GQDs (soybean, 216 mmol/m^2·s; maize, 175 mmol/m^2 s) increased by 6.2% and 4.7% than that of corresponding species without GQDs (soybean, 203 mmol/m^2 s; maize, 167 mmol/m^2·s).

3.3.2. The mechanism for NPAHs adsorption on crop leaf surfaces

The fitting of the experimental results to pseudo-second-order model provided insight into the NPAHs adsorption rates and the nature of chemisorption. However, it is incapable of offering any information about the adsorption mechanism. Generally, the adsorption of adsorbate molecules mainly involves four consecutive stages, which in order are the migration from the bulk of the air to the layer of adsorbent surface, followed by the diffusion through the air layer surrounding the adsorbent, the penetration through the pores on the adsorbent surface, and adsorption on the adsorbent surfaces (Magdy and Altaher, 2018). The second and third stages are considered as the determining steps controlling the adsorption rate since the other two stages are usually fast. The two stages are always studied using film diffusion model (Boyd model) and intra-particle diffusion model (Magdy and Altaher, 2018):

Film diffusion model:

$$B_t = -0.4977 - \ln(1 - q_t/q_e) \quad (4)$$

Intra-particle diffusion:

$$q_t = k_P t^{1/2} + C \quad (5)$$

The means of q_e, q_t (ng/spot) have been given above; B_t is the mathematical function of fractional attainment of equilibrium; k_P represents the rate constant for the intra-particle diffusion model.

For the seedlings without GQDs treatment, it is evident that the line of B_t *versus* t plot exhibited excellent linearity and failed to pass through the origin well (Fig. S5A), indicating that the adsorption process of NPAHs molecules by the crop leaf surfaces was controlled by film diffusion mechanism (Fig. 4a). This adsorption rates decreased with time till reaching the equilibrium and boundary layer resistance might be involved during the initial adsorption stages. However, for the GQDs-treated seedlings, the fitting curves exhibited good linearity and pass through the origin (Fig. S5B), suggesting that film diffusion was not the sole mechanism controlling the adsorption, but intra-particle diffusion played more important role in the rate controlling step due to the addition of GQDs. From the Fig. 3, a sharper region appeared at the early adsorption stage when the GQDs were present, which could be explained by the fast adsorption induced by the electrostatic interaction between the functional groups (*e.g.,* -COOH, -OH) at the outer surface of GQDs and the nitryl-containing NPAH molecules (Fig. 4b). Comparably, the following region was characterized by moderate adsorption, where considerable high R^2 for both of the diffusion models were observed (Table 2). This suggests that the combination of film diffusion and intra-particle diffusion is the dominant mechanism for adsorption processes (Hameed et al., 2008). These findings indicated that the addition of GQDs altered the mechanism for the adsorption kinetics of NPAHs on the crop leaf surfaces.

3.3.3. The q_e of NPAHs on the leaf surfaces

Whether GQDs existed or not, both of 9-NAnt and 3-NFla achieved adsorption equilibrium on the two crop leaf surfaces within the experimental periods of 240 h (Fig. 3). However, compared with the NPAHs without GQDs, the time required to reaching adsorption equilibrium (TAE) was shortened by 15.8–21.7% for the NPAHs coexisted with GQDs. As mentioned above, the presence of GQDs induced a much sharper phase at the initial adsorption stage with less consuming time, which will be a logical explanation for the decreasing TAE. In addition, inter-species and inter-chemical variability existed in terms of the q_e values, as well as the effects of GQDs. For the same crop species, the $q_{e,exp}$ values followed the sequence of 3-NFla > 9-NAnt (Table 2), which should be largely attributed to the facts that the lg K_{OA} values of 3-NFla (10.62) is greater than that of 9-NAnt (9.86) (Musa Bandowe and Meusel, 2017). Generally, greater lg K_{OA} values favor the stronger affinity of adsorbent to the adsorbate (Lin et al., 2007). Within the same chemicals, the q_e of soybean went beyond that of the maize, indicating the soybean leaf surfaces had greater affinity for gaseous NPAHs than the maize. This observation should be closely associated with the more wax content of soybean relative to maize (Sun et al., 2018a).

From Table 2, the q_e values of the two NPAHs increased significantly for either of crop species, since the presence of GQDs not only enlarged the surface area for adsorbing NPAHs, but had superior adsorption performance to the NPAH chemicals due to the electrostatic interaction. Meanwhile, the enhancement degrees varied with different chemicals in the order of 3-NFla (28.7% for soybean, 20.3% for maize) > 9-NAnt (22.8% for soybean, 16.2% for maize), indicating that 3-NFla had the stronger interaction with the functional groups (*e.g.,* -COOH, -OH) at the outer surface of GQDs than 9-NAnt. Logically, the -NO_2 of 3-NFla was more accessible to the outer surfaces of GQDs due to the steric effect (Fig. 4b). In summary, the presence of GQDs promoted the adsorption rates and q_e of NPAHs onto the leaf surfaces of living crop seedlings.

4. Conclusions

In the present work, we successfully developed a novel method for *in situ* determination of NPAHs adsorbed onto the leaf surfaces of living crop seedlings based on the FOF method combined with GQDs as a fluorescent probe. Using the novel approach, the adsorption kinetics of gaseous 9-NAnt and 3-NFla by the living soybean and maize leaf surfaces, as well as the effects of GQDs were investigated *in situ*. The observations yielded some insight into the mechanism for adsorption kinetics of gaseous NPAHs on the crop leaf surfaces for the first time. The presence of GQDs had significant effects on the adsorption kinetics of NPAHs on the crop leaf surfaces, mainly in terms of the TAE and q_e values. In brief, the GQDs decreased the TAE significantly *via* varying the adsorption processes dominated by film diffusion into the mechanism controlled by the combination of film diffusion and intra-particle diffusion. Meanwhile, the presence of GQDs promoted the q_e of NPAHs on the crop leaf surfaces, potentially having an adverse effect on

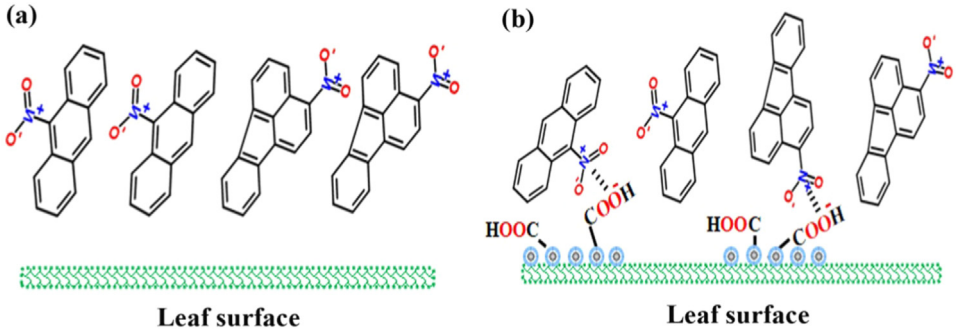

Fig. 4. The interactions between adsorbent surface and NPAH molecules.

agricultural product safety. These findings have significance to an understanding of the environmental processes and fates of NPAHs in crop systems and will enable us to evaluate the crop security more precisely. Furthermore, the interactions of NPAHs with coexisting substances that will likely alter the behaviors, fate and risk in crop system are a valuable and pertinent subject.

Acknowledgments

The authors would like to thank the financial support from the National Natural Science Foundation of China (No. 21507077), Guangzhou Key Laboratory of Environmental Exposure and Health (No. GZKLEEH201609), and Grant from the Central Promotion Plan of Talent Development (rsc1148).

Appendix A. Supporting information

Supplementary data associated with this article can be found in the online version at http://dx.doi.org/10.1016/j.ecoenv.2018.06.059.

References

Achadu, O.J., Nyokong, T., 2017. Graphene quantum dots decorated with maleimide and zinc tetramaleimido-phthalocyanine: application in the design of “OFF-ON” fluorescence sensors for biothiols. Talanta 166, 15–26.
Barber, J.L., Kurt, P.B., Thomas, G.O., Kerstiens, G., Jones, K.C., 2002. Investigation into the importance of the stomatal pathway in the exchange of PCBs between air and plants. Environ. Sci. Technol. 36, 4282–4287.
Chen, C.P., Zhou, W.J., Yang, Q., Zhu, L.F., Zhu, L.Z., 2014. Sorption characteristics of nitrosodiphenylamine (NDPhA) and diphenylamine (DPhA) onto organo-bentonite from aqueous solution. Chem. Eng. J. 240, 487–493.
Chen, H., Gao, B., Li, H., 2015. Removal of sulfamethoxazole and ciprofloxacin from aqueoussolutions by graphene oxide. J. Hazard. Mater. 282, 201–207.
Desalme, D., Binet, P., Chiapusio, G., 2013. Challenges in tracing the fate and effects of atmospheric polycyclic aromatic hydrocarbons deposition in vascular plants. Environ. Sci. Technol. 47, 3967–3981.
Domeño, C., Canellas, E., Alfaro, P., Rodriguez-Lafuente, A., Nerin, C., 2012. Atmospheric pressure gas chromatography with quadrupole time of flight mass spectrometry for simultaneous detection and quantification of polycyclic aromatic hydrocarbons and nitro-polycyclic aromatic hydrocarbons in mosses. J. Chromatogr. A. 1252, 146–154.
Doroodmand, M.M., Deylaminezhad, M., 2015. Electrochemical study on the intercalation properties of hydroxyl anion for the reversible conversion of graphene quantum dots into carbon dots. J. Electroanal. Chem. 756, 161–170.
Fujii, T., Imasaka, T., Imasaka, T., 2017. Use of chemical convention for determination of nitrated aromatic hydrocarbons using femtosecond ionization mass spectrometry. Anal. Chim. Acta 996, 48–53.
Gao, Y., Yang, L.X., Chen, J.M., Li, Y.Y., Jiang, P., Zhang, J.M., Yu, H., Wang, W.X., 2018. Nitro and oxy-PAHs bounded in PM2.5 and PM1.0 under different weather conditions at Mount Tai in Eastern China: sources, long-distance transport, and cancer risk assessment. Sci. Total Environ. 622–623, 1400–1407.
Guiñez, M., Martinez, L.D., Fernandez, L., Cerutti, S., 2017. Dispersive liquid-liquid microextraction based on solidification of floating organic drop and fluorescence detection for the determination of nitrated polycyclic aromatic hydrocarbons in aqueous samples. Microchem. J. 131, 1–8.
Hameed, B.H., Tan, I.A.W., Ahmad, A.L., 2008. Adsorption isotherm, kinetic modeling and mechanism of 2, 4, 6-trichlorophenol on coconut husk-based activated carbon. Chem. Eng. J. 144, 235–244.
Konggidinata, M.I., Chao, B., Lian, Q., Subramaniam, R., Zappi, M., Gang, D.D., 2017. Equilibrium, kinetic and thermodynamic studies for adsorption of BTEX onto ordered mesoporous carbon (OMC). J. Harzard. Mater. 336, 249–259.
Lin, H., Tao, S., Zuo, Q., Conveney, R.M., 2007. Uptake of polycyclic aromatic hydrocarbons by maize plants. Environ. Pollut. 148, 614–619.
Lin, L.P., Rong, M.C., Luo, F., Chen, D.M., Wang, Y.R., Chen, X., 2014. Luminescent graphene quantum dots as new fluorescent materials for environmental and biological applications. TrAC-Trend Anal. Chem. 54, 83–102.
Li, L., Wu, G., Yang, G., Peng, J., Zhao, J., Zhu, J., 2013. Focusing on luminescent graphene quantum dots: current status and future perspectives. Nanoscale 5, 4015–4039.
Li, Q.Q., Chen, B.L., Xing, B.S., 2017. Aggregation kinetics and self-assembly mechanisms of graphene quantum dots in aqueous solutions: cooperative effects of pH and electrolytes. Environ. Sci. Technol. 51, 1364–1376.
Li, R.L., Wang, S.P., Wang, Y.H., Yu, K.F., 2018. Development of a novel methodology for in vivo quantification of N/O/S containing polycyclic aromatic hydrocarbons located on the epidermis of mangrove roots using graphene quantum dots as a fluorescence quencher. Mar. Pollut. Bull. 127, 424–428.
Li, W., Shen, G.F., Yuan, C.Y., Wang, C., Shen, H.Z., Jiang, H., Zhang, Y.Y., Chen, Y.C., Su, S., Tao, S., 2016. The gas/particle partitioning of nitro- and oxy-polycyclic aromatic hydrocarbons in the atmosphere of northern China. Atmos. Environ. 172–173, 66–73.
Liu, X.T., Na, W.D., Liu, H., Su, X.G., 2017. Fluorescence turn-off-on probe based on polypyrrole/graphene quantum composites for selective and sensitive detection of paracetamol and ascorbic acid. Biosens. Bioelectron. 98, 222–226.
Li, Y.G., Chen, B.L., Chen, Z.M., Zhu, L.Z., 2009. Surfactant effects on the affinity of plant cuticles with organic pollutants. J. Agric. Food Chem. 57, 3681–3688.
Li, Y., Hu, Y., Zhao, Y., Shi, G.Q., Deng, L.E., Hou, Y.B., Qu, L.T., 2011. An electrochemical avenue to green-luminescent graphene quantum dots as potential electron-acceptors for photovoltaics. Adv. Mater. 23, 776–780.
Luo, Z.M., Yang, D.L., Yang, C., Wu, X.Y., Hu, Y.L., Zhang, Y., Yuwen, L.H., Yeow, E.K.L., Weng, L.X., Huang, W., Wang, L.H., 2018. Graphene quantum dots modified with adenine for efficient two-photon bioimaging and white light-activated antibacteria. Appl. Surf. Sci. 434, 155–162.
Musa Bandowe, B.A., Meusel, H., 2017. Nitrated polycyclic aromatic hydrocarbons (nitro-PAHs) in the environment - A review. Sci. Total Environ. 581–582, 237–257.
Magdy, Y.H., Altaher, H., 2018. Kinetic analysis of the adsorption of dyes from high strength wastewater on cement kiln dust. J. Environ. Chem. Eng. 6, 834–841.
Sham, A.Y.W., Notley, S.M., 2018. Adsorption of organic dyes from aqueous solutions using surfactant exfoliated graphene. J. Environ. Chem. Eng. 6, 495–504.
Sahub, C., Tuntulani, T., Nhujak, T., Tomapatanaget, B., 2018. Effective biosensor based on graphene quantum dots via enzymatic reaction for directly photoluminescence detection of organophosphate pesticide. Sens. Actuators B. 258, 88–97.
Shehab, M., Ebrahim, S., Soliman, M., 2017. Graphene quantum dots prepared from glucose as optical sensor for glucose. J. Lumin. 184, 110–116.
Su, J., Lin, H., Wang, Q.P., Xie, Z.M., Chen, Z., 2011. Adsorption of phenol from aqueous solutions by organomontmorillonite. Desalination 269, 163–169.
Sun, H.F., Guo, S., Nan, Y.L., Ma, R.Y., 2018a. Direct determination of surfactant effects on the uptake of gaseous parent and alkylated PAHs by crop leaf surfaces. Ecotoxicol. Environ. Saf. 154, 206–213.
Sun, H.F., Feng, R.J., Nan, Y.L., Cheng, Z., Sang, N., 2018b. *In-situ* examination of graphene and graphene oxide impact on the depuration of phenanthrene and fluoranthene adsorbed onto spinach (*Spinacia oleracea* L.) leaf surfaces. Environ. Pollut. 237, 968–976.
Sun, H.F., Shi, J., Guo, S., Zhang, Y., Duan, L.S., 2016. *In situ* determination of the depuration of three- and four-ringed polycyclic aromatic hydrocarbons co-adsorbed onto mangrove leaf surfaces. Environ. Pollut. 208, 688–695.
Sun, H.J., Gao, N., Dong, K., Ren, J.S., Qu, X.G., 2014. Graphene quantum dots-band-aids used for wound disinfection. ACS Nano 8, 6202–6210.
Su, Y.S., Wania, F., 2005. Does the forest filter effect prevent semivolatile organic compounds from reaching the arctic? Environ. Sci. Technol. 39, 7185–7193.
Sun, Z., Zhu, Y., Zhuo, S.J., Liu, W.P., Zeng, E.Y., Wang, X.L., Xing, B.S., Tao, S., 2017. Occurrence of nitro- and oxy-PAHs in agricultural soils in eastern China and excess lifetime cancer risks from human exposure through soil ingestion. Environ. Int. 108, 261–270.
Wang, P., Du, K.Z., Zhu, Y.X., Zhang, Y., 2008. A novel analytical approach for investigation of anthracene adsorption onto mangrove leaves. Talanta 76, 1177–1182.
Wang, S., Zhang, Y.J., Pang, G.S., Zhang, Y.W., Guo, S.J., 2017. Tuning the aggregation/disaggregation behavior of graphene quantum dots by structure-switching aptamer for high-sensitivity fluorescent ochratoxin a sensor. Anal. Chem. 89, 1704–1709.
Yang, X.Y., Liu, S.J., Xu, Y.S., Liu, Y., Chen, L.J., Tang, N., Hayakawa, K., 2017. Emission factors of polycyclic and nitro-polycyclic aromatic hydrocarbons from residential combustion of coal and crop residue pellets. Environ. Pollut. 231, 1265–1273.
Ying, Y.L., He, P., Ding, G.Q., Peng, X.S., 2016. Ultrafast adsorption and selective desorption of aqueous aromatic dyes by graphene sheets modified by graphene quantum dots. Nanotechnology 27, 245703.
Zhu, S.J., Zhang, J.H., Tang, S.J., Qiao, C.Y., Wang, L., Wang, H.Y., Liu, X., Li, B., Li, Y.F., Yu, W.L., Wang, X.F., Sun, H.S., Yang, B., 2012. Surface chemistry routes to modulate the photoluminescence of graphene quantum dots: from fluorescence mechanism to up-conversion bioimaging applications. Adv. Funct. Mater. 22, 4732–4740.
Zhang, Z.P., Zhang, J., Chen, N., Qu, L.T., 2012. Graphene quantum dots: an emerging material for energy-related applications and beyond. Energy Environ. Sci. 5, 8869–8890.